Available online at www.sciencedirect.com
SciVerse ScienceDirect
Ceramics International 38 (2012) 2261–2267
CERAMICS INTERNATIONAL
www.elsevier.com/locate/ceramint

Structural and optoelectronic properties of transparent conductive c-axis-oriented ZnO based multilayer thin films with Ru interlayer

Yuan-Chang Liang *, Xian-Shi Deng, Hua Zhong

Institute of Materials Engineering, National Taiwan Ocean University, 202 Keelung, Taiwan

Received 11 October 2011; received in revised form 11 October 2011; accepted 28 October 2011
Available online 4 November 2011

Abstract

ZnO and Ru multilayer thin films are deposited using the sputtering deposition technique at room temperature. The effects of the Ru interlayer thickness and annealing temperature on the properties of multilayer thin films have been studied. An X-ray diffraction study reveals that ZnO layers are highly *c*-axis-oriented. The use of an Ru interlayer improves the crystalline quality of the subsequently deposited ZnO layers. Moreover, the crystalline quality of the entire structure is further enhanced through thermal annealing in a vacuum. Atomic force microscopy images show that the surface roughness of the multilayer thin films increases with a Ru interlayer thickness greater than 6 nm. The roughness of the film surface increases in correlation with annealing temperatures. This accounts for the decreased optical transmittance of the multilayer thin films annealed at temperatures higher than 450 °C. The electrical resistivity of multilayer thin films decreases with an increase in the metallic interlayer thickness. Thermal annealing at 450 °C causes low resistivity in multilayer thin films. The lowest resistivity reached $\sim 5.4 \times 10^{-4}$ Ω cm for multilayer films with a 10-nm-thick Ru interlayer annealed at 450 °C.

Keywords: A. Films; B. Surfaces; E. Electrodes

1. Introduction

ZnO thin films are wide-band gap N-type semiconductors with high optical transmission across the visible spectrum [1,2]. ZnO thin films have been previously investigated for numerous applications. Among the various applications, ZnO thin films can be used as a transparent conductive oxide layer for several optoelectronic devices, such as flat panel displays and solar cells [3,4]. For applications, ZnO thin films are typically prepared using the sputtering technique because of its large-scale deposition and simple control process [1].

The increasing technological demand for device applications with improved performance necessitates the investigation of ZnO thin films with superior electrical and optical quality. Recently, a ZnO-based multilayer structure containing an ultrathin metal thin film was proposed as an approach to improve the electrical conductivity of ZnO thin films [5]. Several ZnO-based multilayer systems have been reported, such as ZnO/Ag/ZnO, ZnO/Cu/ZnO, and ZnO/Al/ZnO, and these multilayer thin films are fabricated using various vacuum processes [6–8]. The preparation of these ZnO/metal/ZnO multilayer thin films is typically conducted at room temperature and followed with thermal treatments to obtain the optimal electrical and optical properties. However, oxidation of the metal intermediate layers is typically inevitable during thermal annealing because of the metal-oxide interface reaction. Oxidation of the ultrathin metal layer seriously deteriorates the optoelectronic properties of multilayer thin films because ultrathin metal-oxide with high resistivity forms between the ZnO and metal layers. Ru metal, due to its excellent thermal stability, high electrical conductivity, and dry etching compatibility, has been widely used in IC devices [9]. Additionally, its oxide, RuO_2, is also a satisfactory electrical contact material with a low electrical resistivity of ~35 μΩ cm [10]. Recently, the favorable optical properties of RuO_2 were demonstrated by the fabrication of transparent RuO_2 contacts on ZnO thin films. Moreover, the optical transmittance of RuO_2 reaches ~85% [11]. However, research regarding the physical properties of ZnO-based multilayer thin films containing a thin Ru

* Corresponding author. Tel.: +886 2 24622192.
E-mail addresses: yuanvictory@gmail.com, dean1818@gmail.com (Y.-C. Liang).

0272-8842/$36.00
doi:10.1016/j.ceramint.2011.10.076

intermediate layer is lacking. Therefore, this study systemically investigates the effects of Ru interlayer thickness and thermal treatments on the crystal structure and optical and electrical properties of ZnO/Ru/ZnO multilayer thin films formed using the sputtering technique.

2. Experimental procedures

ZnO/Ru/ZnO sandwich structures were sputter deposited on glass (corning 1737) using ZnO and Ru targets. The glass substrates were supersonic clean out in acetone, rinsed in alcohol and subsequently dried in flowing air gas before deposition. The multilayer film deposition was performed with a dual-gun sputtering system with computer control of shutter opening that enabled exact control of the thickness of different layers without breaking the chamber vacuum to change target materials. During the deposition, the substrate temperature was maintained at room temperature and the working pressure is 15 mTorr with a pure Ar atmosphere. The thickness of the ZnO layer was fixed at 40 nm and the thickness of Ru was varied from 4 to 10 nm. A ZnO (40 nm)/Ru (t)/ZnO (40 nm) multilayer structure was constructed. Some of the samples were subsequently annealed by rapid thermal furnace in high vacuum for 1 h at various temperatures (350–650 °C) to investigate the effects of thermal annealing on physical properties of the multilayer thin films.

X-ray diffraction (XRD) with Cu Kα radiation was used to investigate the crystalline quality of the prepared thin films. The surface morphology of the films was investigated with an atomic force microscope (AFM). The binding state of the constituent elements for the sputtering deposited ZnO thin film was evaluated with X-ray photoelectron spectra (XPS) in the Zn 2p and O 1s regions. The composition depth profile was also examined with secondary-ion mass spectrometry (SIMS). Optical transmittance of the prepared samples was measured in the wavelengths of 300–800 nm by using a Shimadzu UV1601 UV-VIS spectrometer. The electrical resistivity was measured by using four-point probe method.

3. Results and discussion

Fig. 1(a) shows XRD patterns of multilayer thin films grown on glass substrates at room temperature. Strong (0 0 2) Bragg reflections from the ZnO layers were observed, indicating that the ZnO layers in multilayer structures possess a *c*-axis-textured orientation. ZnO thin films grown on glass substrates using sputtering deposition at room temperature have been reported to possess a (0 0 2)-preferred crystallographic orientation under adequate processing conditions [12]. Ru thin films have been demonstrated to be an excellent template for growing *c*-axis-oriented ZnO thin films [13]. No Bragg reflections were observed in the Ru interlayer. This could be because the Ru interlayer is too thin to provide a strong Bragg diffraction, and/or the crystallinity of the ultrathin Ru is not sufficient to display an intense Bragg reflection. Notably, the peak intensity increases and the full width at half maximum (FWHM) of ZnO Bragg reflections decreases with an increase

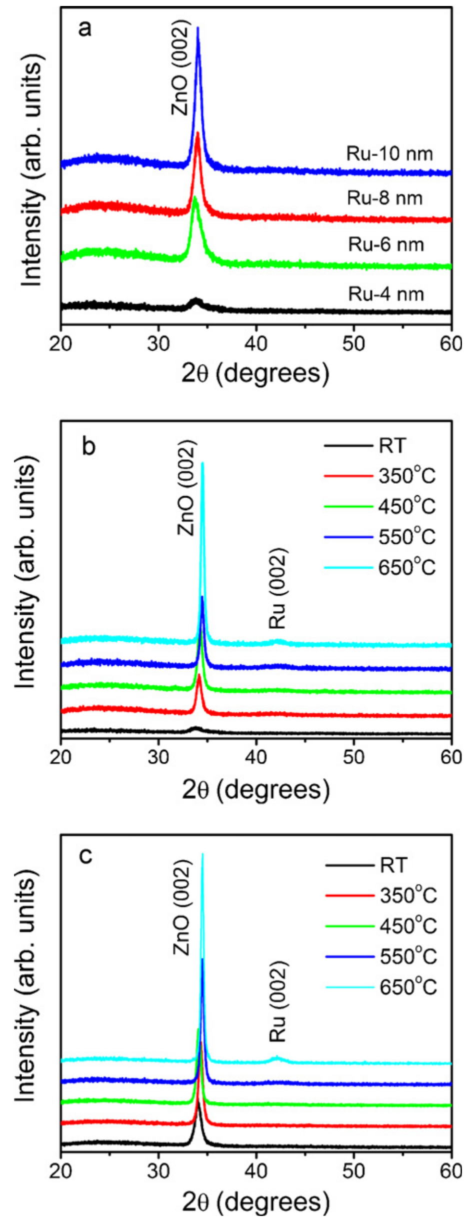

Fig. 1. (a) XRD patterns of the multilayered films grown on glass substrates at room temperature. (b) XRD patterns for the multilayer thin films with a 4 nm-thick Ru interlayer annealed at various temperatures. (c) XRD patterns for the multilayer thin films with a 10 nm-thick Ru interlayer annealed at various temperatures. (For interpretation of the references to color in the artwork, the reader is referred to the web version of the article.)

in Ru interlayer thickness. This finding indicates that a thicker Ru interlayer increases the degree of crystallinity of the subsequently deposited ZnO layers. A similar phenomenon has been exhibited by ZnO thin films grown on Ag metal layers [6]. The peak positions of the ZnO (0 0 2) Bragg reflection (located at 33.7–34.01°) are lower than that of the standard ZnO referenced from JCPD No. 89-1397 (34.38°). Lattice expansion in oxide thin films has been attributed to an oxygen vacancy in the lattice [14]. The sputtering growth of oxide thin films in oxygen-deficient ambient has been proven to significantly affect the lattice constant of oxide thin films [14,15]. The effects of annealing temperatures on the microstructures of

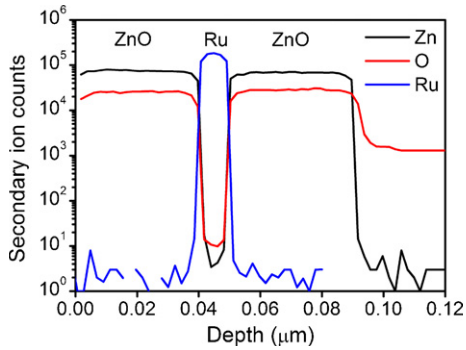

Fig. 2. SIMS depth profiling of the ZnO (40 nm)/Ru (8 nm)/ZnO (40 nm) multilayer film. (For interpretation of the references to color in the artwork, the reader is referred to the web version of the article.)

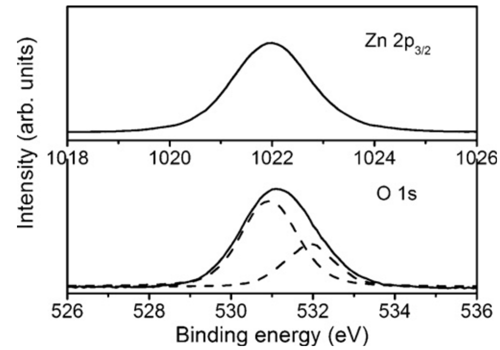

Fig. 3. XPS narrow scans of the sputter-deposited ZnO film: (a) Zn 2p spectrum and (b) O 1s spectrum.

multilayer thin films were also examined using XRD. The representative XRD patterns for multilayer thin films with an Ru interlayer thicknesses of 4 and 10 nm are shown in Fig. 1(b) and (c). Greater peak intensity of the ZnO Bragg reflections was observed following annealing at higher temperatures, revealing an enhanced crystalline quality in ZnO thin films. Additionally, the decreased FWHM value of the ZnO Bragg reflections in correlation with the annealing temperature may indicate that the grain size of ZnO films increased under higher annealing temperatures. Similar temperature-dependent microstructure evolution was observed in the ultrathin Ru interlayer. The Bragg reflection of the Ru (0 0 2) becomes apparent at high annealing temperatures. This agrees with the findings in related literature, namely that the enhancement of the quality and grain size of metallic thin films is strongly associated with the thermal process temperature [16].

The composition modulations in the as-deposited ZnO (40 nm)/Ru (8 nm)/ZnO (40 nm) multilayer thin film on the glass were examined with SIMS depth profiles. The results are shown in Fig. 2, in which the variation of signals of the respective elements is consistent with the designed structure. Fig. 3 shows the chemical bonding states of the Zn and O elements in the sputtering deposited ZnO thin film on the Ru interlayer. The XPS curve of Zn $2p_{3/2}$ was centered at ~1021.95 eV and this value is close to the reported value of Zn^{2+} in ZnO film [17]. Moreover, Fig. 3(b) shows the O1s spectrum consists of two well defined curves. This is resulted from the non-stoichiometry of oxygen element in ZnO. The higher binding energy component represents oxygen ions in oxygen-deficient regions within the matrix of ZnO [10]. The similar result is observed in the sputter-deposited semiconductor oxide films prepared in oxygen-deficient ambient [14,18].

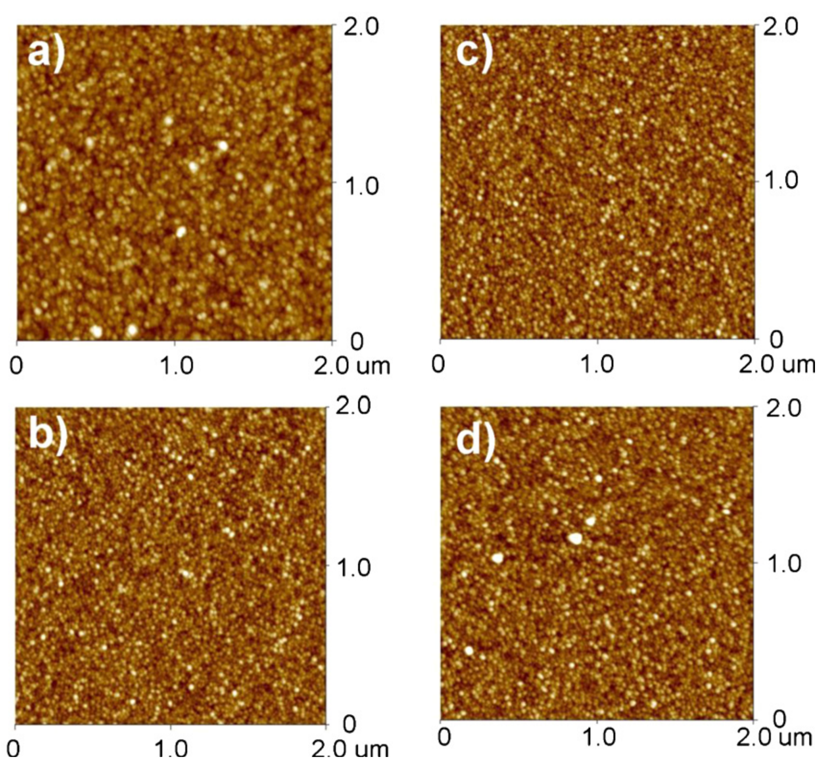

Fig. 4. AFM surface images of the multilayer thin films with various Ru interlayer thicknesses grown at room temperature.

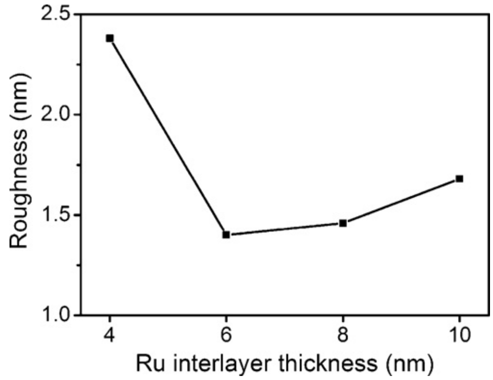

Fig. 5. Surface roughness of the multilayer thin films evaluated from the AFM images shown in Fig. 4.

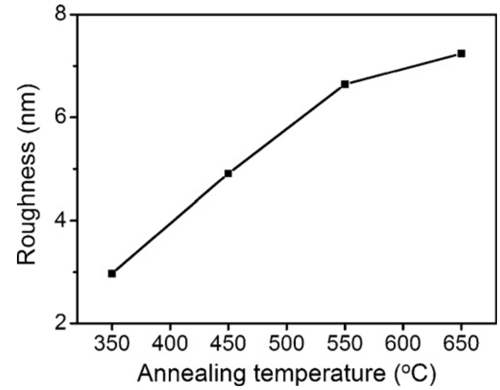

Fig. 7. Surface roughness of the multilayer thin films evaluated from the AFM images shown in Fig. 6.

Fig. 4 shows the AFM images of the multilayer thin films possessing various Ru interlayer thicknesses grown at room temperature. Fig. 5 displays the film surface roughness evaluated from the AFM images shown in Fig. 4. In this study, the multilayer thin films with a 4-nm-thick Ru interlayer possessed the greatest root-mean-square (rms) surface roughness (2.38 nm). Numerous large ZnO crystals formed on the area of interest. This could be because the sputtering-deposited Ru interlayer was too thin (4 nm) to provide uniform nucleation sites for the growth of the ZnO top layer subsequently deposited. The surface roughness increases with greater Ru interlayer thickness (>6 nm). Multilayer films with a 6-nm-thick Ru interlayer had a rms surface roughness of 1.4 nm, whereas films with a 10-nm-thick Ru interlayer had a 1.68 nm surface roughness. AFM images of the effects of annealing temperatures on the surface morphology of multilayer thin films with an 8-nm-thick Ru interlayer are shown in Fig. 6; varying rms surface roughness is displayed in Fig. 7. AFM images of a sample annealed at 350 °C reveal that the film surface exhibits a clear dual grain-size distribution. However, a number of relatively large grains were found to be non-uniformly distributed among the tiny surface grains. The surface grains of the films further coarsen under higher annealing temperatures. Finally, large and separately distributed surface grains were observed on the film surface after the substrate was annealed at 650 °C. A higher annealing temperature initially causes coarser surface grains, which roughens the surface of multilayer thin films. The surface morphology evolution of thin films has been demonstrated to be significantly affected by thermal treatments [19]. A similar result for other multilayer transparent oxide films containing a metallic interlayer has been reported [20]. The peak-to-valley roughness (*p–v*) is defined as the vertical distance between the highest and lowest points. The *p–v* value of films is proposed to possess a

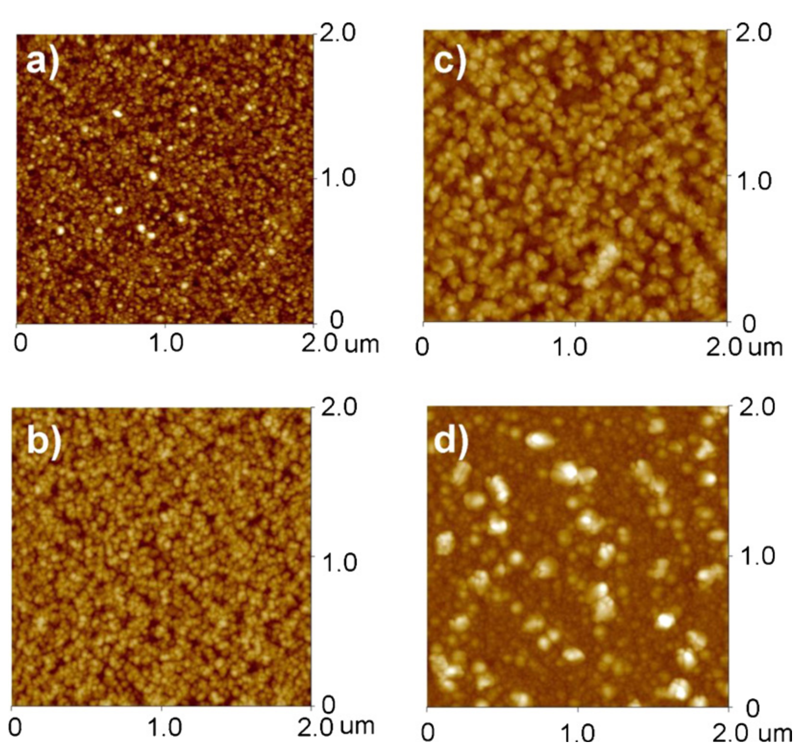

Fig. 6. AFM images for the multilayer thin films with an 8 nm-thick Ru interlayer annealed at various temperatures.

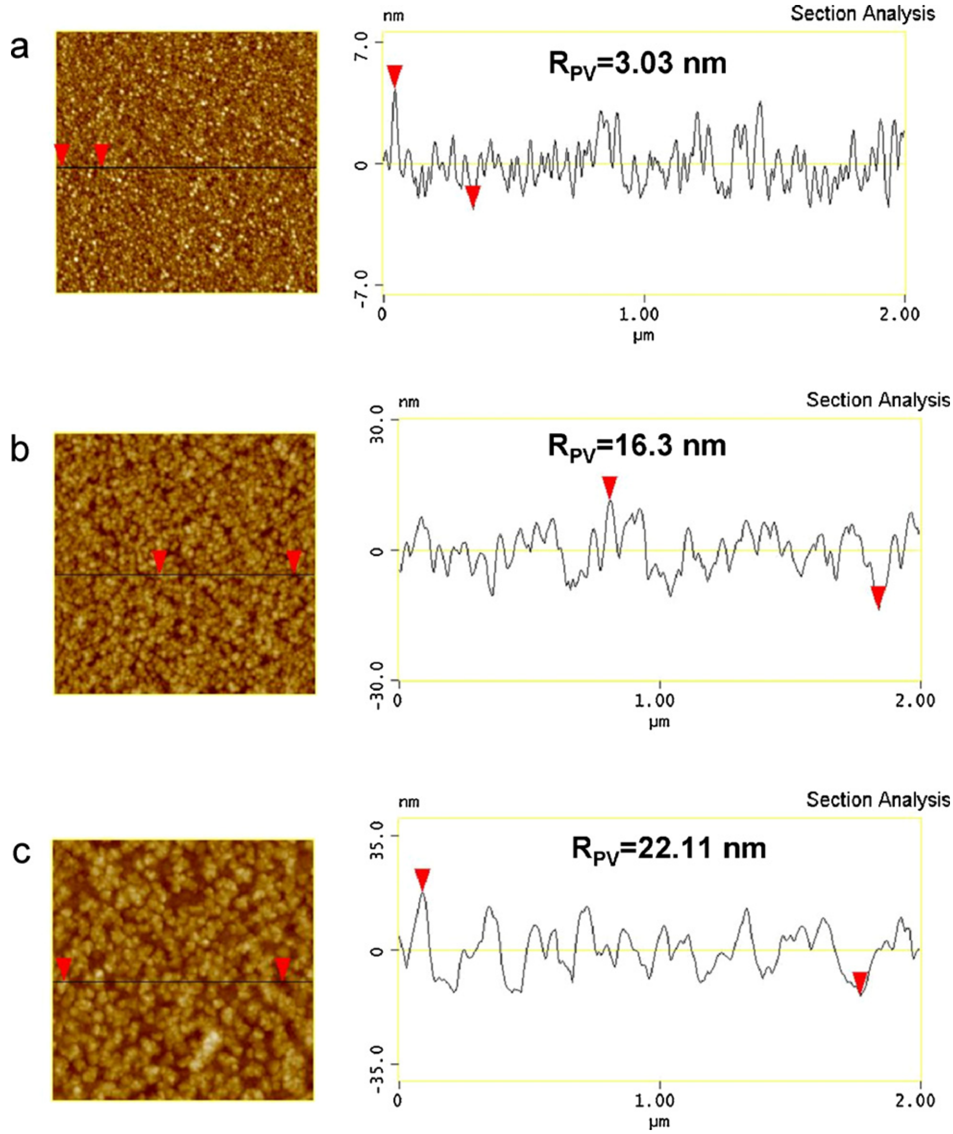

Fig. 8. AFM section analysis for the peak-valley value of the multilayer films with an 8 nm-thick Ru interlayer annealed at various temperatures: (a) room temperature, (b) 450 °C and (c) 550 °C.

linear relationship with the reverse leakage current of devices [12]. Fig. 8 shows the effects of thermal annealing on the *p–v* value of multilayer films with an 8-nm-thick Ru interlayer. Multilayer film with an 8-nm-thick Ru interlayer has a *p–v* value of 3.03 nm; the films annealed at 450 °C and 550 °C have a *p–v* value of 16.3 nm and 22.11 nm, respectively. Increasing the annealing temperature dramatically increases the *p–v* value of films. This is because of the annealing temperature-dependent evolution of the grain size of multilayer film surfaces.

Fig. 9 shows the representative optical transmittance of multilayer thin films with and without thermal annealing at 450 and 650 °C. Fig. 9(a) shows a multilayer film with a 4-nm-thick Ru interlayer, which has the lowest average optical transmittance in the visible wavelength region. This is due to the poor crystalline quality of the multilayer film, as revealed by the XRD result. Multilayer films with a 6-nm- and 8-nm-thick Ru interlayer have an average optical transmittance of approximately 75.1% and 76.5% (Fig. 9(d)), respectively. When further increasing the Ru interlayer thickness to 10 nm, the average optical transmittance declines to approximately 65.5% because the thicker metallic layer hinders transmittance of incident light [5]. The effects of the thermal annealing temperature on the optical transmittance of multilayer thin films are displayed in Fig. 9(b) and (c). Notably, the optical transmittance in all the multilayer film variations was enhanced by annealing at 450 °C. The average optical transmittance of multilayer films with an 8-nm-thick Ru interlayer reached 85.4% (Fig. 9(d)). However, upon further increasing the annealing temperature to 650 °C, the optical transmittance of multilayer thin films declined. Both the crystalline quality and surface roughness of multilayer thin films might affect the optical transmittance. A higher crystalline quality of the film will increase the optical transmittance; whereas a rougher film surface will scatter the incident light, further decreasing the optical transmittance [21,22]. AFM measurements have shown that higher annealing temperatures increase the surface grain size of thin films,

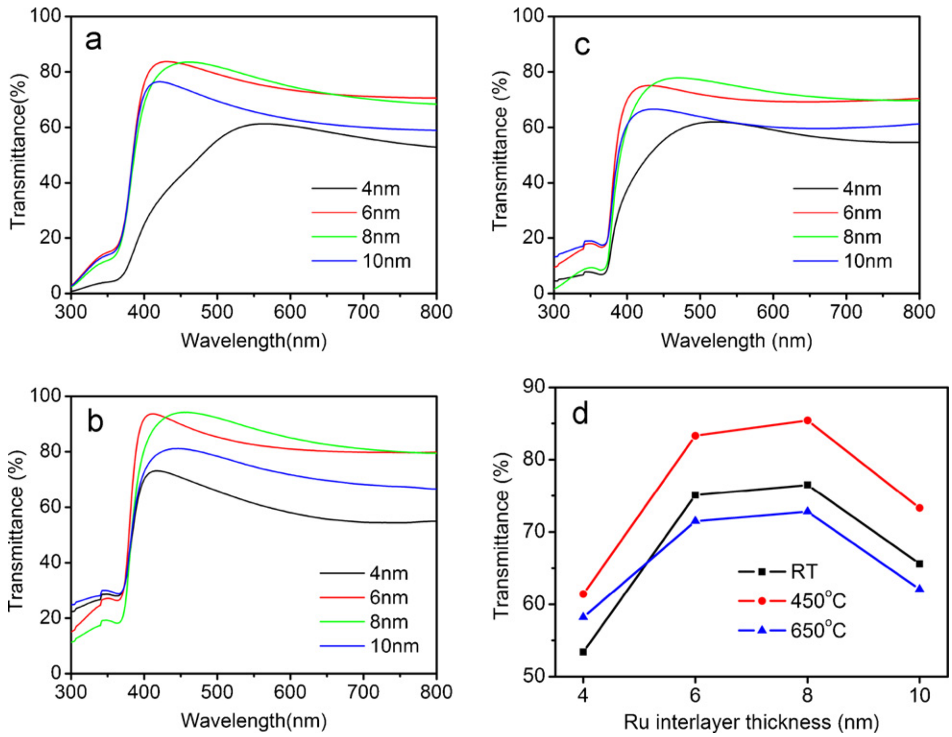

Fig. 9. . Optical transmittance spectra of the multilayer films with and without thermal annealing: (a) without annealing, (b) annealed at 450 °C, (c) annealed at 650 °C and (d) average optical transmittance of the multilayer thin films in the visible wavelength region. (For interpretation of the references to color in the artwork, the reader is referred to the web version of the article.)

further roughening the film surface. The enhanced optical transmittance under an annealing temperature of 450 °C might be associated with a substantial improvement in the crystalline quality of films. Moreover, a rough film surface may account for the decreased optical transmittance of multilayer thin films annealed at the high temperature of 650 °C.

Fig. 10 shows the electrical resistivity dependence of multilayer thin films annealed at various temperatures. An obvious decline in resistivity was observed in multilayer films with a metallic interlayer thicker than 4 nm. This clearly indicates that the metallic interlayer is significant to the electrical conductance of the entire structure. The electrical resistivity of multilayer thin films decreases with

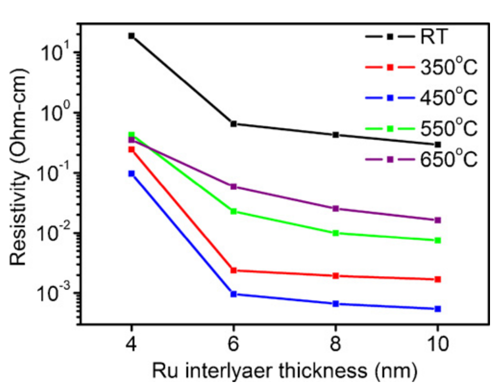

Fig. 10. Electrical resistivity of the multilayer thin films annealed at various temperatures. (For interpretation of the references to color in the artwork, the reader is referred to the web version of the article.)

an increase in the metallic interlayer thickness. The resistivity of multilayer thin films further decreases with annealing temperatures of 450 °C. The improved crystallinity in both the ZnO and Ru layers accounts for the observed results. A lower resistivity was observed in multilayer films with a 6–10-nm-thick Ru interlayer annealed at 450 °C. The lowest resistivity reached $\sim 5.4 \times 10^{-4}\ \Omega$ cm for multilayer films with a 10-nm-thick Ru interlayer annealed at 450 °C. However, a higher annealing temperature (>550 °C) did not further improve the electrical conductance of multilayer films. This might be because high annealing temperatures induce the formation of ultrathin RuO_x between the ZnO/Ru interface. RuO_x, though a metal-oxide, possesses a higher resistivity than Ru metal does. Additionally, the formation of RuO_x could roughen the interface of the metal-oxide layers [23]. Both reasons might account for the decreased electrical conductance of the entire structure. Deteriorated electrical and optical properties due to a roughened interface between the constituent layers have been reported in silver/indium–tin oxide multilayer thin films [24]. Notably, the use of Ag and Al metallic interlayers in multilayer structures significantly decreased electrical conductance (greater than as-deposited films) when the samples were annealed at high temperatures. This is attributed to the oxidation of the metallic layer with ZnO during high temperature annealing [6,8]. Comparatively, though an Ru metallic interlayer can oxidize at high annealing temperatures, the metallic nature of RuO_x decreases the resistivity of the as-deposited multilayer thin films.

4. Conclusions

ZnO/Ru/ZnO multilayer thin films were sputter-deposited on glass substrates at room temperature. The ZnO layers were highly *c*-axis-oriented in the multilayer structure, and the crystalline quality of the films improved through thermal annealing in a vacuum. Both the surface roughness and peak-to-valley roughness increased under annealing temperatures. The average optical transmittance of multilayer thin films in the visible wavelength region decreases with an Ru interlayer thickness greater than 6 nm. The average optical transmittance of multilayer thin films increases with annealing temperatures of 450 °C because of the enhanced crystalline quality of the films. However, further increasing the annealing temperature to 650 °C decreased the optical transmittance of the film surface. The electrical resistivity of multilayer thin films decreases with an increase in the thickness of the metallic interlayer. The decreased electrical resistivity of multilayer thin films annealed under a temperature of 450 °C is attributed to the improved crystallinity of the films. Further increasing the annealing temperature decreases the electrical conductance of films because of the possible oxidation of the Ru metallic interlayer and rough ZnO/Ru interface. Based on the experimental results, the best-performing multilayer thin film is ZnO (40 nm)/Ru (8 nm)/ZnO (40 nm) annealed at 450 °C, which possesses a high average optical transmittance of 85.4% and an electrical resistivity of $\sim 6.6 \times 10^{-4}\ \Omega$ cm.

Acknowledgements

This work is supported by the National Science Council of the Republic of China (Grant nos. NSC 100-2221-E-019-059-MY2 and NSC 100-2628-E-019-003-MY2) and National Taiwan Ocean University (Grant no. NTOU-RD-AA-2010-104031).

References

[1] Y.C. Liang, Growth and characterization of nonpolar *a*-plane ZnO films on perovskite oxides with thin homointerlayer, J. Alloys Compd. 508 (2010) 158–161.
[2] Y.J. Chen, Y.Y. Shih, C.H. Ho, J.H. Du, Y.P. Fu, Effect of temperature on lateral growth of ZnO grains grown by MOCVD, Ceram. Int. 36 (2010) 69–73.
[3] A.M. Gheidar, E.A. Soleimani, Structural properties of indium tin oxide thin films prepared for application in solar cells, Mater. Res. Bull. 40 (2005) 1303–1307.
[4] M. Fahland, P. Karlsson, C. Charton, Low resisitivity transparent electrodes for displays on polymer substrates, Thin Solid Films 392 (2001) 334–337.
[5] J. Lou, M. Bao, B.J. Ye, H.M. Weng, H.J. Du, Z.B. Zhang, The design of transparent conductive ZnO/metal/ZnO multilayers for incidence from 0° to 70°, J. Opt. A: Pure Appl. Opt. 11 (2009) 085501–085505.
[6] D.R. Sahu, S.Y. Lin, J.L. Huang, Investigation of conductive and transparent Al-doped ZnO/Ag/Al-doped ZnO multilayer coatings by electron beam evaporation, Thin Solid Films 516 (2008) 4728–4732.
[7] D.R. Sahu, J.L. Huang, Dependence of film thickness on the electrical and optical properties of ZnO–Cu–ZnO multilayers, Appl. Surf. Sci. 253 (2006) 915–918.
[8] M.F. Al-Kuhaili, M.A. Al-Maghrabi, S.M.A. Durrani, I.A. Bakhtiari, Investigation of ZnO/Al/ZnO multilayers as transparent conducting coatings, J. Phys. D: Appl. Phys. 41 (2008) 215302–215305.
[9] T. Nabatame, M. Hiratani, M. Kadoshima, Y. Shimamoto, Y. Matsui, Y. Ohji, I. Asano, T. Fujiwara, T. Suzuki, Properties of Ruthenium films prepared by liquid source metalorganic chemical vapor deposition using $Ru(EtCp)_2$ with tetrahydrofuran solvent, Jpn. J. Appl. Phys. 39 (2000) L1188–L1190.
[10] Y.C. Liang, M.Y. Tsai, C.L. Huang, C.Y. Hu, C.S. Hwang, Structural and optical properties of electrodeposited ZnO thin films on conductive RuO_2 oxides, J. Alloys Compd. 509 (2011) 3559–3565.
[11] T.K. Lin, S.J. Chang, B.R. Huang, K.T. Lam, Y.S. Sun, M. Fujita, Y. Horikoshi, Transparent RuO_x Contacts on n-ZnO, J. Electrochem. Soc. 153 (2006) G677–G680.
[12] Y.C. Liang, C.C. Liu, C.C. Kuo, Y.C. Liang, Structural and opto-electronic properties of transparent conducting (2 2 2)-textured Zr-doped In_2O_3/ZnO bilayer films, J. Crystal Growth 310 (2008) 3741–3745.
[13] W.T. Lim, C.H. Lee, Highly oriented ZnO thin films deposited on Ru/Si substrates, Thin Solid Films 353 (1999) 12–15.
[14] Y.C. Liang, Y.C. Liang, Physical properties of low temperature sputtering-deposited zirconium-doped indium oxide films at various oxygen partial pressures, Appl. Phys. A: Mater. Sci. Process. 97 (2009) 249–255.
[15] Y.C. Liang, Hydrogen-induced degradation in physical properties of dielectric-enhanced $Ba_{0.6}Sr_{0.4}TiO_3/SrTiO_3$ artificial superlattices, Electrochem. Solid State Lett. 13 (2010) G91–G94.
[16] T. Suzuki, Y. Abe, M. Kawamura, K. Sasaki, T. Shouzu, K. Kawamata, Optical and electrical properties of pure Ag and Ag-based alloy thin films prepared by RF magnetron sputtering, Vacuum 66 (2002) 501–504.
[17] L. Zhang, Z. Chen, Y. Tang, Z. Jia, Low temperature cathodic electrodeposition of nanocrystalline zinc oxide thin films, Thin Solid Films 492 (2005) 24–29.
[18] Y.C. Liang, H.Y. Lee, Growth of epitaxial zirconium-doped indium oxide (2 2 2) at low temperature by rf sputtering, CrystEngComm 12 (2010) 3172–3176.
[19] Z.B. Fang, Z.J. Yan, Y.S. Tan, X.Q. Liu, Y.Y. Wang, Influence of post-annealing treatment on the structure properties of ZnO films, Appl. Surf. Sci. 241 (2005) 303–308.
[20] D.R. Sahu, J.L. Huang, The properties of ZnO/Cu/ZnO multilayer films before and after annealing in the different atmosphere, Thin Solid Films 516 (2007) 208–211.
[21] Y.C. Liang, Y.C. Liang, Buffering effect on physical properties of transparent $BaTiO_3$ capacitors on composite transparent electrodes, Scripta Mater. 61 (2009) 117–120.
[22] Y.C. Liang, Thickness dependence of structural and electrical properties of electric field tunable $Ba_{0.6}Sr_{0.4}TiO_3$ transparent capacitors, Electrochem. Solid-State Lett. 12 (2009) G54–G56.
[23] J.H. Huang, Y.S. Lai, J.S. Chen, Comparison of dielectric characteristics of Ta_2O_5 thin films on RuO_2 and Ru bottom electrodes, J. Electrochem. Soc. 148 (2001) F133–F136.
[24] A. Klöppel, W. Kriegseis, B.K. Meyer, A. Scharmann, C. Daube, J. Stollenwerk, J. Trube, Dependence of the electrical and optical behaviour of ITO–silver–ITO multilayers on the silver properties, Thin Solid Films 365 (2000) 139–146.